LUND
UNIVERSITY

Indoor and Outdoor Measurements of Particulate Matter with the Low-Cost Optical Sensor OPC-N3

Author
Ellen Soroka

Supervisor
Erik Ahlberg

Co-Supervisor
Adam Kristensson

Co-Supervisor
Johannes Ekdahl du Rietz

Bachelor of Science

Department of Nuclear Physics

Spring Semester 2020

Abstract

This paper evaluates the low-cost optical sensor OPC-N3 from Alphasense as a suitable scientific instrument for measuring particulate matter levels in air, both outdoors and indoors. The time-keeping and data-retrieval was additionally improved by connecting the OPC-N3 to an Arduino microcontroller equipped with a real-time clock (RTC) module and an external SD card. Inter-comparison tests demonstrated good agreement between four co-located sensors, with approximately 15% relative standard deviation (RSD) before separation for indoor and outdoor measurements, and 13% after. The RSD was observed to increase during periods of very high and very low concentration. Indoor and outdoor measurements were run over 10 days, during which the times of relevant activities were logged. The median ratio of indoor to outdoor concentration was found to be 0.37 for PM_1, 0.44 for $PM_{2.5}$, and 0.53 for PM_{10}. Time series of PM_1, $PM_{2.5}$, and PM_{10} mass concentrations displayed considerably clear trends in accordance with activities, most notably cooking, burning candles, and vaping outdoors. While the indoor particulate matter concentration was generally lower than outdoors, indoor activities appeared to have a more significant contribution to the concentration of particulate matter than recorded outdoor sources. The accuracy of the sensors was additionally evaluated through comparison of PM_{10} values from the outdoor sensors and from Lund Municipality's TEOM instrument, which resulted in a reasonable correlation (median ratio of 1.15) despite the instruments not being co-located. The OPC-N3 sensor was deemed to be a sufficiently precise sensor for detecting trends in particulate matter concentrations, and a good tool for extending the spatial and temporal resolution of air quality monitoring networks. The results of this paper prompt the need for further research to give a more comprehensive evaluation of the OPC-N3, namely, longer measurement periods to evaluate seasonal variation and possible accumulation of errors, a more controlled analysis of sensor response to individual indoor sources, and co-location of the OPC-N3 with reference particulate matter measurement instruments.

Acknowledgements

Firstly, I would like to express my gratitude to my supervisors for taking their time to help and guide me through this project. I am especially grateful to Erik Ahlberg for introducing me to the field of aerosols and low-cost sensors, and for thoroughly explaining concepts and answering my questions. I am also grateful to Johannes Ekdahl du Rietz for patiently assisting me with the electronics and programming aspects. Secondly, I would like to thank Mårten Spanne from Malmö Stad, who provided me with information regarding the Lund reference data. Finally, special thanks to my parents who have supported and encouraged me throughout the course of my bachelors studies.

Contents

List of Abbreviations

EU	European Union
FDMS	Filter Dynamic Measurement System
LED	Light Emitting Diode
OPC	Optical Particle Counter
PM	Particulate Matter
PSL	Polystyrene Spherical Latex Particles
RI	Refractive Index
RSD	Relative Standard Deviation
RTC	Real Time Clock
SPI	Serial Peripheral Interface
SS	Slave Select
TEOM	Tapered Element Oscillating Microbalance
WHO	World Health Organisation

Chapter 1

Introduction

1.1 Particulate Matter

Particulate matter, otherwise known as aerosol particles, refers to the solid and liquid particles of varying composition, size, and origin, which are suspended in air. The size of these particles varies from the nanometer scale to several tens of microns (Hinds, 1982). Although there are some natural sources, anthropogenic sources have led to particulate matter becoming a major air pollutant with detrimental consequences to human health and the environment. Based on guidelines and models from the World Health Organization (WHO) (2016), approximately 90% of the human population is exposed to unclean air, representing the biggest environmental risk to human health, with outdoor air pollution alone causing around 3 million premature deaths globally each year. Poor air quality is not only limited to outdoors; indoor air quality is affected by pollutants from outdoors as well as sources indoors. However, there is a lack of quantitative understanding of indoor sources of particulate matter, accompanied by a lack of regulations for indoor exposure (Koivisto et al., 2019).

1.1.1 Formation and Sources of Particulate Matter

Particulate matter is formed in two ways: primary particles are emitted directly to the atmosphere, while secondary particles form in the atmosphere from gaseous pollutants. In the latter, precursor pollutant gases can condensate onto pre-existing particles, or form new particles through nucleation. There are many natural sources of particulate matter, such as wind-borne dust, sea spray, and pollen. The predominant anthropogenic sources are fossil fuel combustion, agricultural processes, and industrial emissions. Indoors, aerosol particles can be generated by activities such as cooking, burning candles, cleaning or cosmetic aerosol sprays, wood-fires, vacuuming, and the general re-suspension of dust due to movement. Additionally, the infiltration of outdoor air occurs through doors, windows, and gaps around them, as well as either natural or mechanical ventilation.

1.1.2 Properties of Particulate Matter

Particulate matter varies in shape: suspended liquid particles are predominantly approximately spherical, while solid aerosol particles exist in more non-uniform shapes. However, measurement techniques and models often have to assume the particles are spherical, assigning an equivalent diameter such that the resulting sphere retains the same physical attributes of the irregular particle. The aerodynamic diameter is the equivalent diameter of a spherical particle with standard particle density ($1000\,\mathrm{kg/m^3}$) and the same settling velocity of the irregular particle, and is the primary property used to describe particle size.

When measuring, regulating, and monitoring particulate matter, it is usually grouped into two size fractions: PM_{10} and $PM_{2.5}$, which represent coarse particles with an aerodynamic diameter less than $10\,\mu m$, and fine particles less than $2.5\,\mu m$, respectively. Ultra-fine

particles less than 0.1 µm ($PM_{0.1}$) are sometimes classified separately.

Particulate matter is most commonly measured by mass concentration. This is the mass of particulate matter in a unit volume of aerosol, usually with units g/m^3. The number concentration is another property commonly measured, differing from mass concentration since smaller particles contribute more to particle numbers than mass, and vice versa for larger particles.

1.1.3 Effects on Health and Environment

There is strong epidemiological evidence that exposure to air pollution leads to acute lower respiratory infection, chronic obstructive pulmonary disease, ischeamic heart disease, stroke, and lung cancer (WHO, 2016). There are many other acute and chronic health ailments which have been linked to particulate air pollution, including conditions impacting the central nervous system and cognitive ability (Concas et al., 2019). The size of the particles roughly determines how harmful they will be, since the smaller they are, the easier they can penetrate deep into the airways and lodge in the lungs (Valavanidis et al., 2008).

Considering some studies (European Commission, 2003; Klepeis et al., 2001) suggest the average person spends 85–90% of their time indoors, the sources and effects of indoor particulate matter is particularly important. Generally, levels inside are expected to be lower than outside, provided there are no major sources such as smoking indoors. Less is known about the effects of specifically indoor particulate matter pollution, in part due to the inherent challenge of measuring and regulating people's private residences. The price, portability, and useability of low-cost sensors can help to fill this knowledge gap, for example with the application to citizen scientists participating in air quality networks.

Another reason for the interest in monitoring particulate matter is its affect on the climate. Particulate matter interacts in the atmosphere in complex ways and consequently there is a high degree of uncertainty surrounding aerosol-cloud interactions and related effects on radiative forcing (Intergovernmental Panel on Climate Change, 2013). Even though some particles like black carbon (soot) absorb sunlight and cause Earth's atmosphere to warm, there is likely a net cooling effect on the climate, since other particles can increase the Earth's albedo and reflect solar radiation away from Earth. Consequently, models show that the total removal of aerosol particles of anthropogenic origin from the atmosphere would cause the Earth to warm by 0.7 °C (Samset et al., 2018).

The European Union (EU) limits ambient $PM_{2.5}$ exposure to 25 $\mu g/m^3$ per year, and daily PM_{10} exposure to 50 $\mu g/m^3$ or annually 40 $\mu g/m^3$ (European Environment Agency, 2016). WHO (2006) regulations are even stricter, with $PM_{2.5}$ exposure limited to 25 $\mu g/m^3$ per day or 10 $\mu g/m^3$ yearly, while the PM_{10} yearly limit is reduced to 20 $\mu g/m^3$. However, there are currently no equivalent regulations or global standards for indoor concentrations of particulate pollutants.

1.2 Measuring Particulate Matter

Given the health and climate-related consequences, measuring and monitoring particulate matter is highly important. The European Standard 12341:2014 describes the recommended reference method for measuring $PM_{2.5}$ and PM_{10} mass concentration as the gravimetric measurement method (Swedish Standards Institute, 2020). This method involves sampling the particulate matter on filters over 24 hours, before weighing them on a mass balance. It is validated for measuring particles in the range of 1–150 µg/m^3 for PM_{10} and 1–120 µg/m^3 for $PM_{2.5}$. However, other methods can be used for official air quality monitoring if they are deemed to be equivalent under standard conditions, possibly with a correction factor applied.

An example of an equivalent instrument is the Tapered Element Oscillating Microbalance (TEOM). This instrument measures the mass concentration of aerosol particles using a small, hollow glass tube which oscillates at different frequencies depending on how much its inertia is changed by the mass of the deposited particles. Since the TEOM can be sensitive to humidity and temperature fluctuations, it requires a heated inlet to minimise the deposition of water droplets on the filter. Heating the sample can also cause some semi-volatile components of the particulate mass to be removed, which can be corrected for with the addition of a Filter Dynamic Measurement System (FDMS) module.

1.2.1 Optical Measurement of Particulate Matter

Aside from gravimetric instruments, optical techniques can be used to measure concentrations of particulate matter, since scattered light can be detected for particles as small as 0.1 µm. Compared to other methods, optical instruments can provide continuous, instantaneous measurements, with information on the size distribution of the particles and minimal disturbance to the aerosol. The main disadvantage of optical instruments is the sensitivity of scattering to slight variations in particle size or shape, refractive index (RI), or the scattering angle (Hinds, 1982).

The mode of scattering depends on the diameter of the particle. Below 0.05 µm, Rayleigh scattering is predominant, while above around 100 µm, geometric optics can describe the scattering. In the middle range, elastic scattering of light according to the more complicated Mie theory dominates. Mie scattering is the generalised solution to Maxwell's equations, describing the scattering of light through a homogeneous spherical medium with a different RI than the surrounding medium (Acharya, 2017). This occurs when the particle diameter is approximately equal to or larger than the wavelength of the incident light, such as is the case for most aerosol particles. In optical instruments, when a particle passes in front of the light source (usually a laser beam), some light is scattered towards the sensor which registers an intensity based on the particle's diameter. The larger the particle, the wider the peak in intensity will be. As long as the air flow is constant, the diameter of the particle can be estimated and subsequently used to calculate the mass concentration in the air.

1.2.2 Low-cost Sensors

The methods described above may result in high accuracy and precision, but the instruments themselves are relatively large and expensive (Njalsson and Novosselov, 2018). Therefore, they often lack the spatial and sometimes temporal resolution required to understand and assess particulate matter levels on the local scale, where they tend to be more inhomogeneous (Holstius et al., 2013). Low-cost sensors for measuring air quality are emerging as alternatives or additions to traditional methods and resulting in the area of research surrounding them quickly expanding. Firstly, by being more affordable, a greater number of sensors can be deployed in networks of sensors. Their smaller size, portability, and useability are of additional benefit. However, while these aspects are improved, there may be a trade-off in the quality of the data (Yuval et al., 2019). The European Commissions' review of air quality monitoring sensors (Karagulian et al., 2019) cautions low-cost sensors' susceptibility to atmospheric conditions and levels of pollution concentration, only accepting good agreement with reference measurements when the coefficient of determination, R^2, is greater than 0.75 and the slope of regression line is within 1 ± 0.5.

1.2.3 OPC-N3

The low-cost sensor used in this study is the OPC-N3 (Optical Particle Counter) released in January 2019 by Alphasense. The OPC-N3 is sold for €338 at the time of writing, which is comparatively more expensive than other particulate matter sensors on the market from manufacturers such as Plantower, Winsen, and Nova Fitness, which can be as cheap as €15–€30 (Karagulian et al., 2019). The higher price of the OPC-N3 is justified by its wider range of particle size classification, the use of a laser as opposed to light emitting diodes (LEDs), and larger measurement chamber. Considering the reference and equivalent instruments used in environmental monitoring stations can cost hundreds of thousands of euros, the OPC-N3 is still considered a low-cost sensor.

As the name suggests, the OPC-N3 uses optics to detect, size, and count particulate matter. A class 1 diode laser [1] with wavelength 658 nm is scattered by particles drawn into the sensor through a 7 mm inlet with the help of a motorised fan. All particles are represented with a spherical equivalent size regardless of their shape, akin to most other OPCs. Polystyrene Spherical Latex (PSL) particles with known diameter and RI are used in calibration since these properties allow the scattering to be predicted with Mie theory.

The sensor can sort and count particles into 24 bins according to their size, between a range of 0.3 µm and 40 µm. The particle size histogram data is then automatically used to calculate the mass of particulate matter per unit volume of air (µg/m^3) for PM_1, $PM_{2.5}$ and PM_{10}. This calculation assumes a default particle density of 1.65 g/cm^3 and RI = 1.5. Table 1.1 below displays some of the specifications of the OPC-N3.

[1] Class 1 lasers are considered safe under normal operating conditions. The OPC does not contain any user-serviceable parts and therefore the user should never experience direct exposure to the laser while it remains enclosed within the device.

Table 1.1: *Technical specification of the OPC-N3.*

Specification	**Value**
Particle range	0.35–40 µm
Maximum particle count rate	10 000 particles/s
Detection limit (PM_{10})	0.01 µg/m^3–1500 mg/m^3
Sample flow rate	280 mL/min
Current, measurement mode	180 mA (<45 mA in standby)
Temperature range	-10–50 °C
Humidity range	0–95%
Weight	<105 g

This model is an update of the original OPC-N2 sensor, developed at the Centre for Atmospheric and Instrumentation Research at the University of Hertfordshire. The two models are similar with regards to specifications, however the OPC-N3 has an increased particle detection range, and improved laminar flow, allowing the sensor to stay cleaner in highly polluted environments (Alphasense, 2018). As the OPC-N3 is relatively new there are naturally fewer pre-exisiting published studies evaluating its accuracy.

Studies performed with the OPC-N2 model have yielded varied results. The OPC-N2 has been observed to overestimate the output when RH is above 80–90% (Badura et al., 2018), a result of water vapor condensing on particulate matter in high RH environments, increasing their size and mass (Feinberg et al., 2018). Crilley et al. (2018) reported measurements within 33% of TEOM-FDMS data after correction for relative humidity (RH), while inter-comparison of 14 sensors gave a precision of 22 ± 13% for PM_{10}, concluding that, "they would be suitable devices for applications where the spatial variability in particle concentration was to be determined". Alternatively, Badura et al. (2018) found that without RH correction, the OPC-N2 sensors displayed only moderate precision, with a RSD = 20%, and an overestimation of TEOM data by a factor of 4.5–5. In a comparison to low-cost sensor models by Plantower, Bulot et al. (2019) found the OPC-N2 showed more variability across three measurement locations, possibly reflecting a higher precision and, "better capacity to measure short-term localised events or be linked to external environmental factors".

Since the OPC-N3 alone is unable to attach a time-stamp to the data it records, the user is required to write down the start and stop time, and manually extrapolate the time-stamps in between. Problems can arise with this method when the sensor loses power, which is known to occur in the field, particularly in remote areas. This project improves the time-keeping capabilities of the OPC-N3 sensor to combat this issue by connecting an Arduino micro-controller so that the integration of a RTC can be facilitated.

Alphasense recommends the OPC-N3 for use in measuring both indoor and outdoor particulate matter concentrations. After the addition of a time-stamp, the precision of the sensor will be tested by co-locating four units. Furthermore, its ability to distinguish between different particle source–activities in indoor and outdoor environments will be evaluated.

Chapter 2

Method

2.1 Connecting the Arduino and RTC

This section describes the process of connecting a RTC to the OPC-N3 via Arduino. This allows each measurement taken by the sensor to be saved with a timestamp, which is particularly useful when analysing results from several sensors, and if the power is interrupted during measurements. An added benefit of collecting data through the Arduino and SD card is that the OPC-N3 can easily be used with Apple and Unix operating systems, whereas the Alphasense software can only be run by computers running Windows.

2.1.1 Electronic Components

An Arduino UNO micro-controller board was used to connect and program the RTC and the OPC-N3. A PCF8523 model RTC is pre-assembled on the Data Logger Shield from Adafruit, which is a modular circuit board also containing a SD card and a CR1220 coin cell battery. The RTC is a 'I2C' device, meaning two wires are used for communication: the serial clock (SCL) and serial data (SDA). The device uses a 32.768 kHz quartz crystal for time-keeping, and the coin cell battery allows the RTC to continuously record the current time even when the Arduino looses power (Earl, 2020). Without the RTC, the Arduino is only capable of counting the number of milliseconds since it was last powered. The OPC and Arduino were connected via a 6-pin serial peripheral interface (SPI).

2.1.2 Assembly

To connect the shield to the Arduino, 0.1" male headers were soldered to the shield, as well as a 2×3 female header to connect to the Arduino's ICSP (In-Circuit Serial Programming) pins. Two resistors of 220 Ω and 150 Ω were soldered directly to the prototyping area on the shield so that voltage to the SS pin would be reduced to 3.3 V. The SPI wires were also soldered directly to the prototyping area on the shield. The two user-configurable LEDs on the shield were connected to pins 2 and 3 and coded to turn on if an error occurred with the SD card or file.

Figure 1: *OPC-N3 wired to the Arduino and data logger shield.*

2.1.3 Code

To program the date and time to the RTC, the Arduino library RTClib.h from Adafruit was installed. This allowed the RTC to adopt the current time and date of the computer when the sketch [1] was compiled. To allow communication between the Arduino and the OPC, a sketch was provided by Alphasense and modified to accommodate communication to the RTC and SD card. The original Arduino sketch programmed the sensor to take ten 1-second measurements in a 1-minute cycle, and rest the fan and laser during the remainder of the period, thereby maximising the lifetime of the sensor. This code was modified so that the sensor would continually record data every second as long as it was connected to power. Furthermore, the sketch was modified so that the time and date would be appended to the beginning of each row of data. The data was saved in comma separated text files.

2.2 Measurements and Analysis

This section describes the set-up of measurements for inter-comparison of sensors and comparison of indoor and outdoor air. The measurement location was a ground-floor, 68 m^2 apartment with two residents, located in a student housing area in Lund, Sweden (55°43'N, 13°13'E). Four sensors were placed in pairs in waterproof, plastic electrical boxes with holes for the sensor inlets to draw in air (fig. 14). Placing two sensors in almost identical conditions allowed for a more accurate inter-comparison of their precision. The box also had an open tube on one side for pressure equalisation, in order to maintain constant air flow as the sensor fan continually draws in air. The indoors measurement location was a central location in the apartment hallway, at approximately head height. Outdoors, the sensors were placed on an open-backed shelf close to the front door, also at around head height. Figure 2 illustrates the floor plan and placement of the sensors. RH and temperature were measured with the OPC-N3's internal sensors.

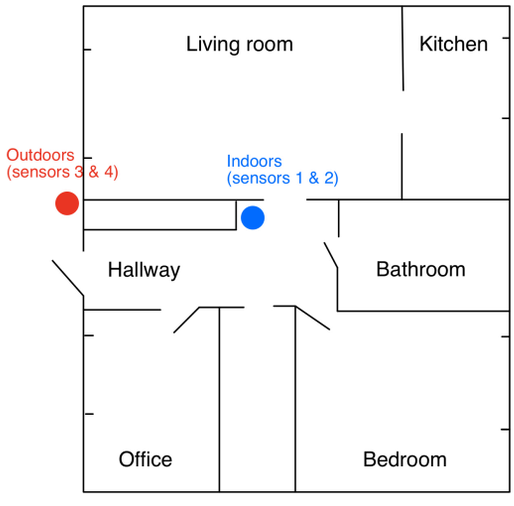

Figure 2: *Floor plan of apartment showing placement of sensors.*

[1] 'Sketch' is the Arduino name for a program.

2.2.1 Inter-comparison Tests

Inter-comparison tests were performed with co-located sensors both before and after separating them for the main run of measurements, to check the degree of agreement between the four sensors. The four sensors were placed adjacent (within their casing) at the indoor measurement location. The first test was run before the indoor/outdoor measurements, and the second co-location test followed after those measurements were completed.

Inter-comparison analysis of the data from the four sensors was performed in Matlab. Time series of both sets of data from all sensors were produced with averages over suitable time periods. Linear regression analysis was applied to compare each sensor to the median of all four sensors, for PM_1, $PM_{2.5}$, and PM_{10}. The median was calculated rather than the average to minimise the effect of outliers. The RSD of each data point was plotted as a time series and an average value was determined for each PM concentration value.

2.2.2 Measurements Indoors and Outdoors

After the first co-location test, two sensors (labelled sensors 1 and 2) were kept indoors, while the other two (sensors 3 and 4) were moved to the outdoor measurement location. The sensors were run for 10 days without intentional power interruption. During this time, a log of activities was kept along with the relevant times. Activities recorded were cooking (frying, boiling, or baking), vacuuming, vaping (outdoors), burning candles, showering, and leaving and returning to the apartment.

For the data collected in this main measurement campaign, time series were produced for the mass concentration of PM_1, $PM_{2.5}$ and PM_{10} with both 10 minute and 1 hour averages. Time series plots were also produced with the average of the two indoor sensors and the average of the two outdoor sensors, again with both 10-minute and 1-hour resolution. The 10-minute averaged time series were compared with the log of activities to ascertain whether there was a correlation between certain activities and increases in particulate matter concentration.

Finally, the averaged hourly outdoor concentration of PM_{10} was compared to official Lund measurements over the same time period. In Lund, official PM_{10} data is measured by the local environmental government agency (Miljöförvaltningen) with a TEOM 1400ab located at street-level (3 m above ground) on Trelleborgsvägen, west of the Lund Central train station. A time series plot was produced and the ratio between the datasets was also calculated and plotted against time. Additionally, a scatter plot of the outdoor OPC readings against the Lund TEOM data was produced to assess their agreement.

Chapter 3

Results and Discussion

3.1 Inter-comparison of Sensors

The co-located measurements before and after the indoor and outdoor measurements displayed relatively good agreement between sensors. However, the time series showed one sensor was measuring noticeably lower concentrations compared to the others in both inter-comparison tests.

The first inter-comparison test was performed overnight, when particulate matter concentrations are generally reduced, since particulates have a chance to settle without movement causing re-suspension. However, the time series includes a significant peak of high concentration for all sizes, due to a period of vaping indoors. The time of the vaping episode (04:10–05:10) matched with significant increases in the relative standard deviations for all size fractions, as shown in the following figures 3–5, indicating that the precision of the sensors suffered at high particle mass concentration. With the vaping event included, the median %RSD values were 8.0%, 9.6%, and 16.7% for PM_1, $PM_{2.5}$, and PM_{10} respectively.

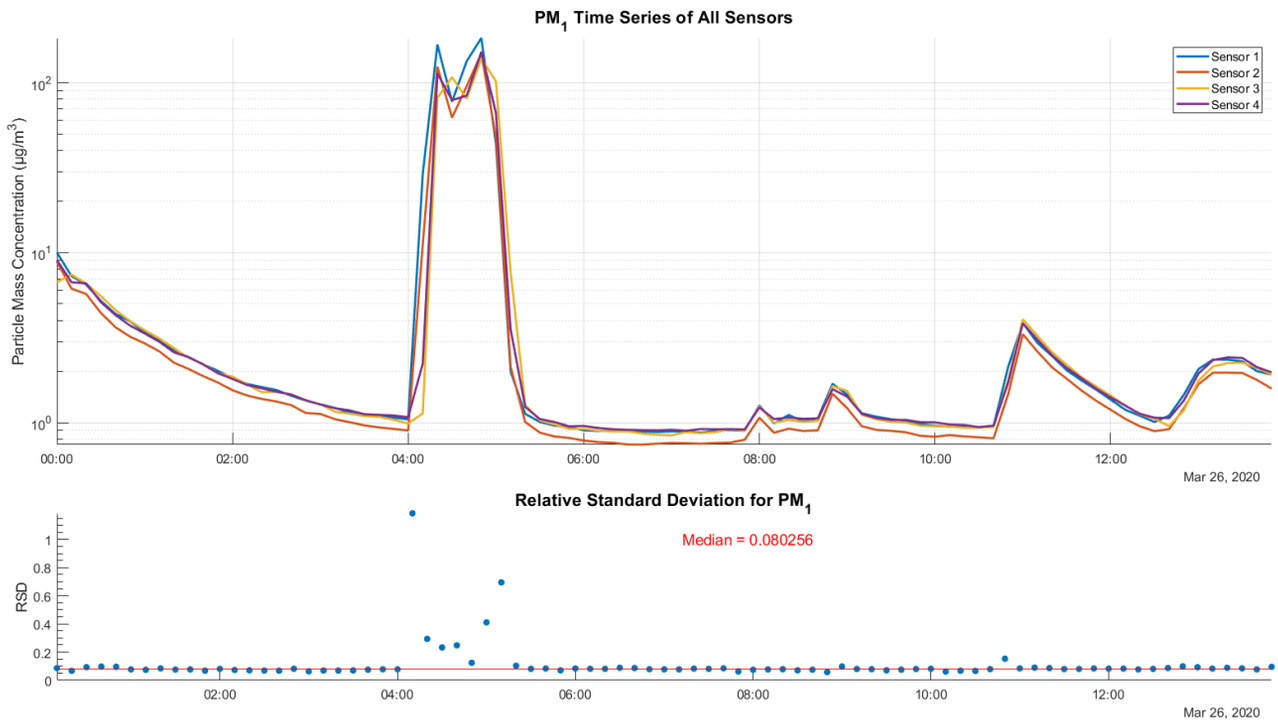

Figure 3: *Time series of PM_1 in the first co-location test with 10-minute averages and the RSD over time.*

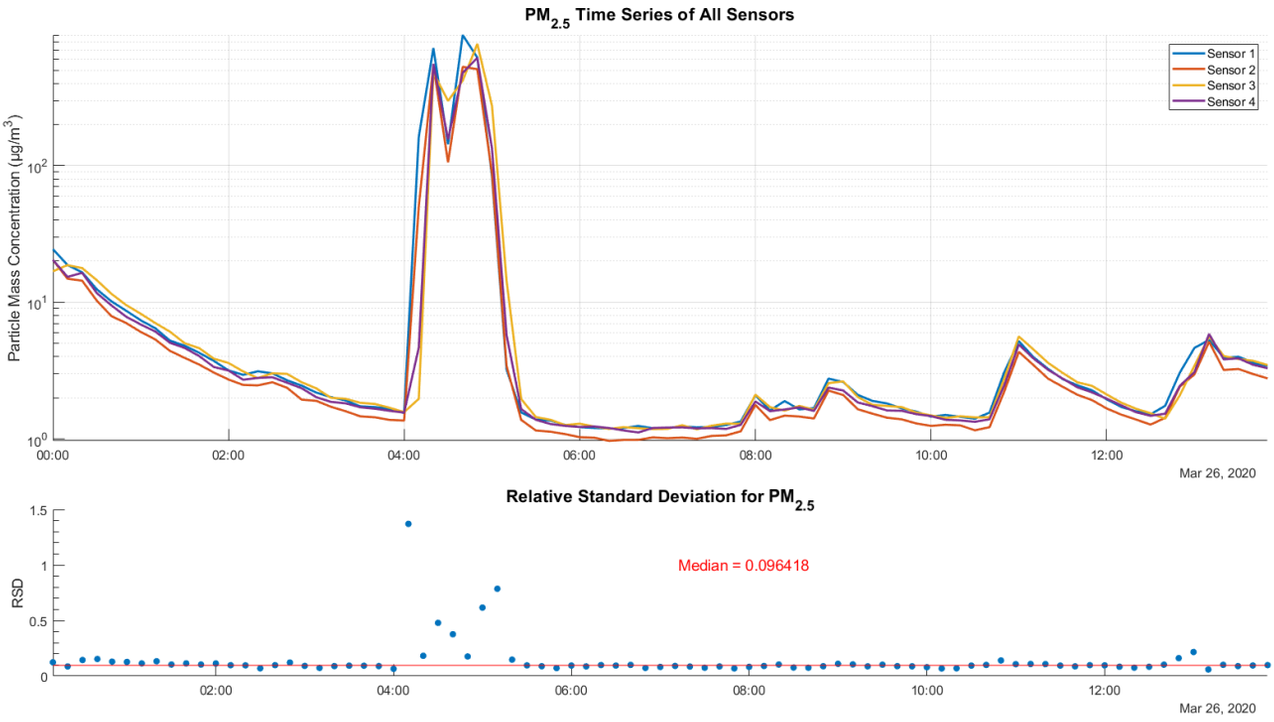

Figure 4: *Time series of $PM_{2.5}$ in the first co-location test with 10-minute averages and the RSD over time.*

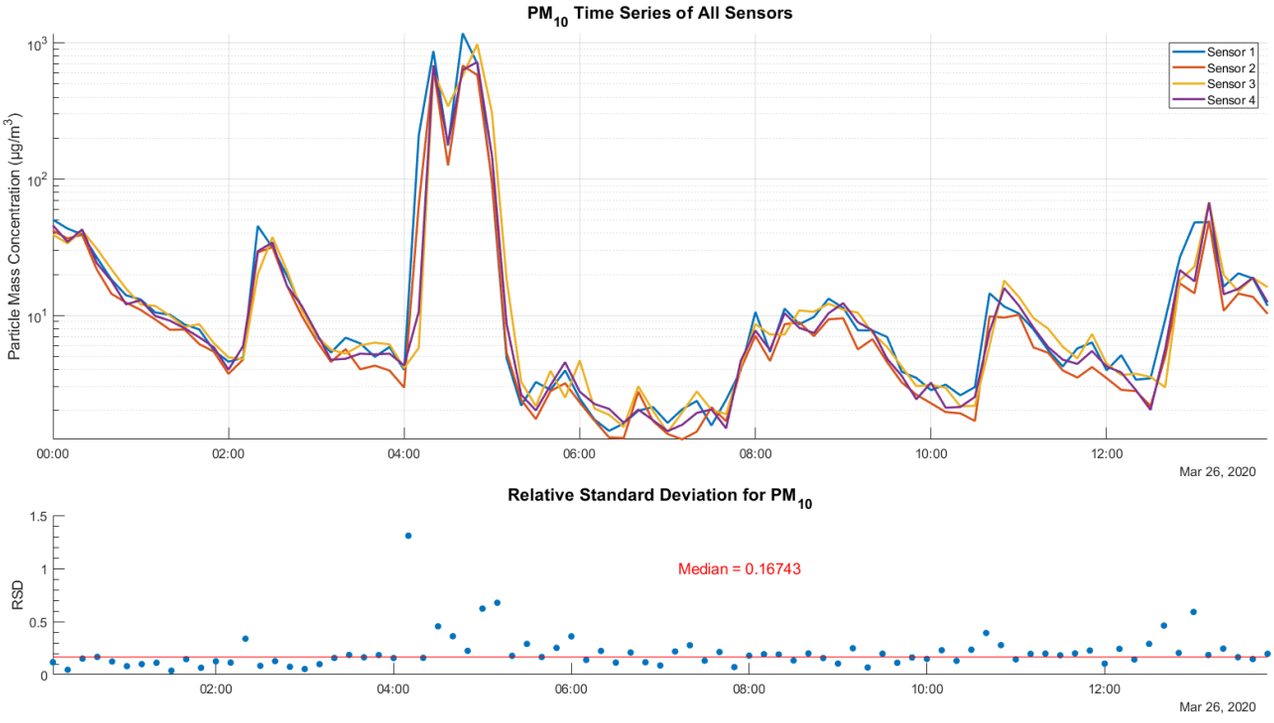

Figure 5: *Time series of PM_{10} in the first co-location test with 10-minute averages and the RSD over time.*

Particulate matter from vaping devices has typically been found to have aerodynamic

diameters in the range of 0.25–0.45 µm (Ingebrethsen et al., 2012). Even though this extends below the official lower detection limit of the OPC-N3, it is not impossible for some particles to be detected below 0.35 µm, due to the lognormal size distribution. Alphasense has measured that the sensor detects 100% of particles at 0.35 µm and 50% at 0.3 µm. Therefore, the sensor likely detects some percentage of smaller particles such as those produced in vaping, although with a significant underestimation.

Sensor 2 proved to be measuring mass concentrations consistently below the other three sensors. This was confirmed in the linear regression analysis, where the data points were aligned along a smaller slope. The linear regression results for $PM_{2.5}$ are shown below in figure 6 as an example, and the similar results for PM_1 and PM_{10} can be found in the appendix (fig. 15–16). Linear regression for sensor 1 did result in a linear fit with a notably higher slope than the other sensors, which appears to be due to this sensor overestimating during peak concentrations.

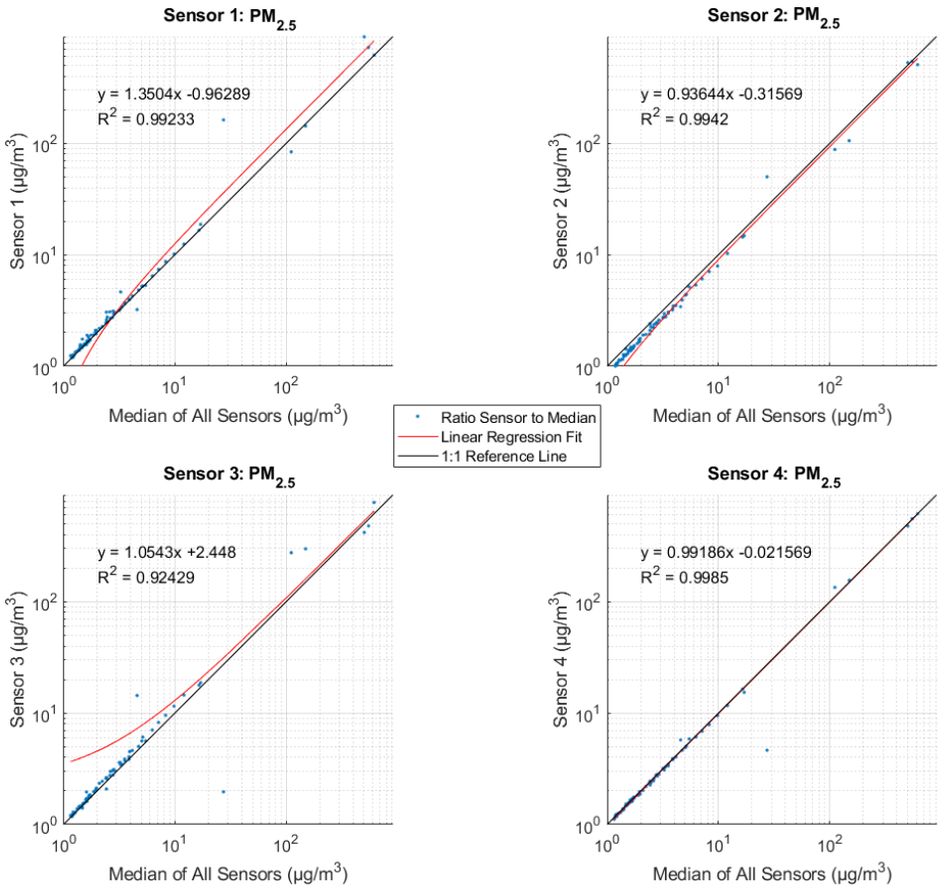

Figure 6: *Linear regression fit of each sensor's $PM_{2.5}$ readings in the first co-location test against the median of all four sensors, with 1:1 line as reference.*

The data points for all four sensors are mostly located very close to the 1:1 reference line. Sensor 4 showed the best correlation to the median of all sensors, although there were some outlying values. The regression line should logically pass through the origin, but in

some cases the intercept reached almost 2.5. The corresponding slopes were close to 1, but the non-zero intercepts indicate that the relation is non-linear at low concentrations. Note that the log-log scale used to better visualise the spread of data causes the line to bend.

The second co-located measurements spanned a longer time, so there were more peaks in general, reaching concentrations comparable to the time series in the first test. However, unlike the vaping episode, it was the periods of low concentration which caused some high RSD values, particularly within PM_{10} readings (fig. 9). The median %RSD values were still found to be 11.9%, 11.8%, and 13.8% for PM_1, $PM_{2.5}$, and PM_{10} respectively in the second co-location test. Both inter-comparison tests therefore resulted in a higher degree of precision (lower RSD) compared to the "moderate" result (20%) from the OPC-N2 sensors tested by Badura et al. (2018).

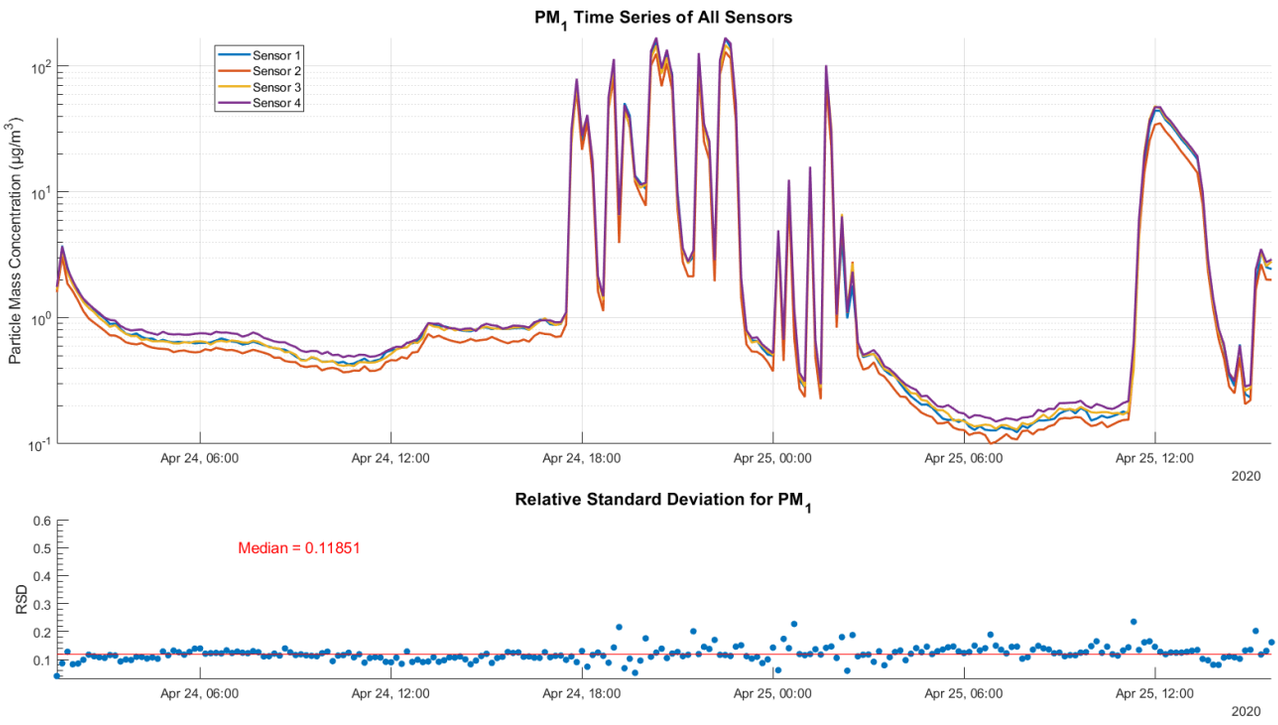

Figure 7: *Time series of PM_1 in the second co-location test with 10-minute averages and the RSD over time.*

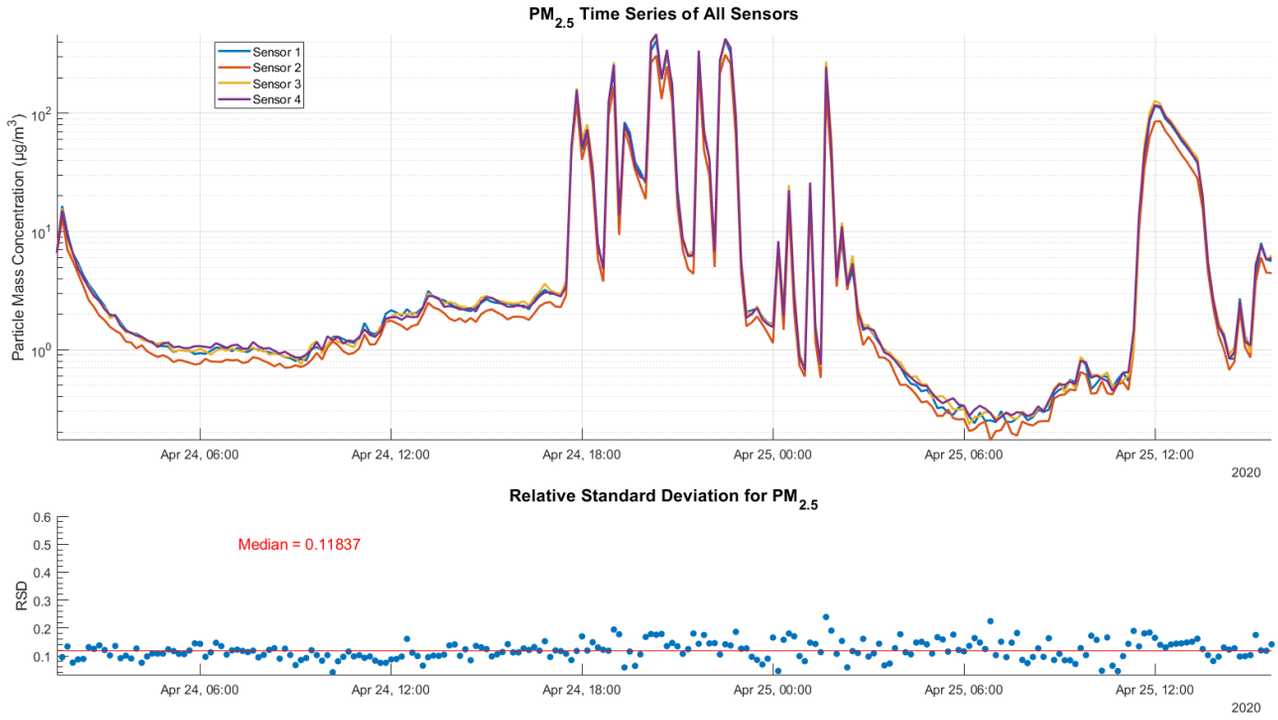

Figure 8: *Time series of $PM_{2.5}$ in the second co-location test with 10-minute averages and the RSD over time.*

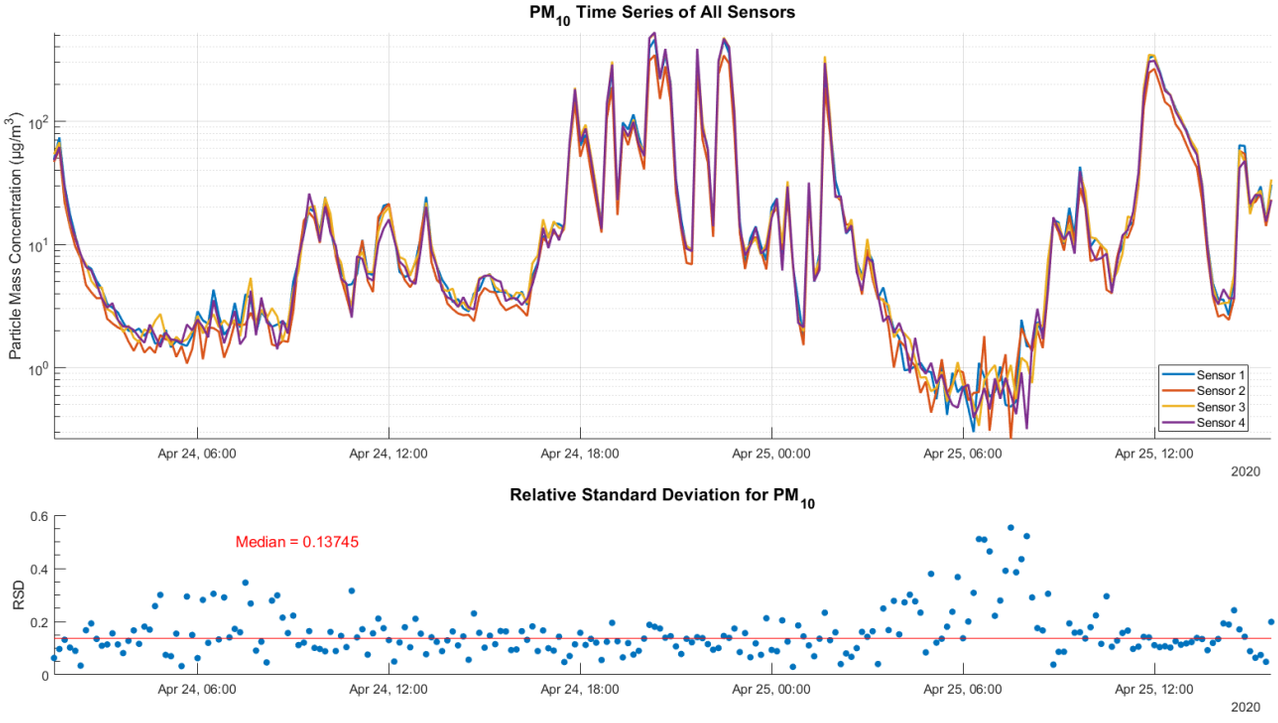

Figure 9: *Time series of PM_{10} in the second co-location test with 10-minute averages and the RSD over time.*

In the second inter-comparison test, the time series also suggested that sensor 2 was recording lower values than the other sensors. The slope of the linear regression fit for

sensor 2 was approximately 25% below the other sensors. The result for $PM_{2.5}$ is again shown as an example in figure 10, while similar results for PM_1 and PM_{10} are found in the appendix (fig. 17-18).

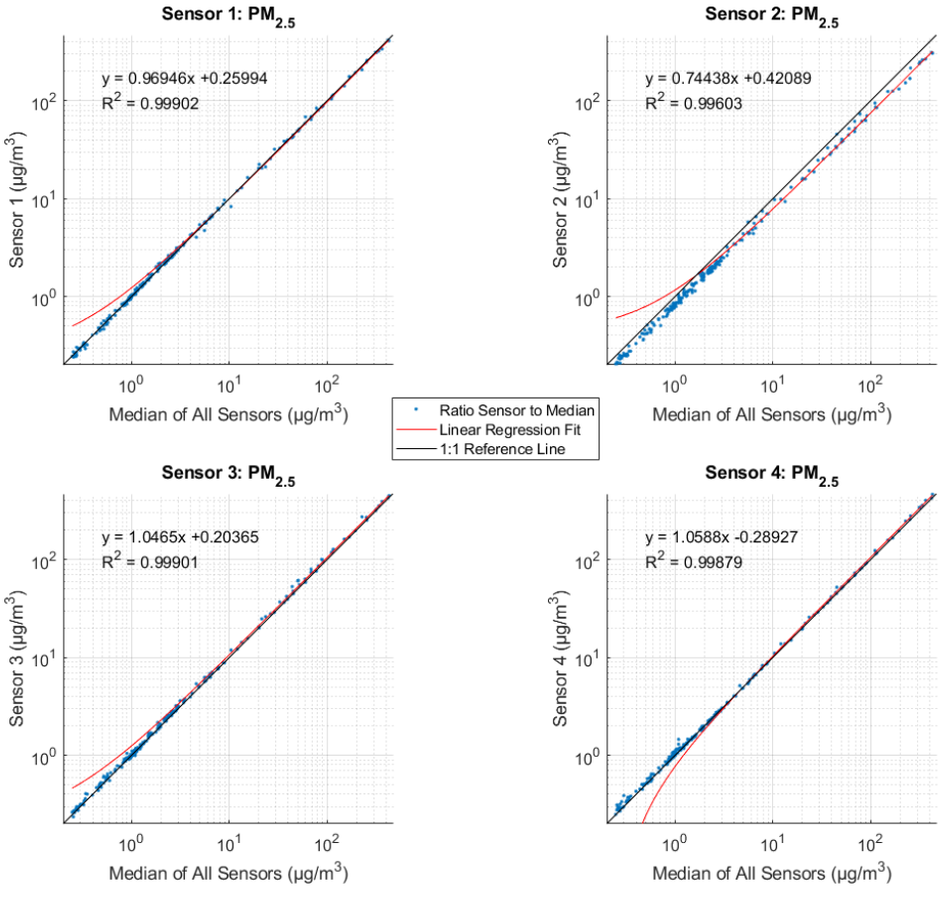

Figure 10: *Linear regression fit of each sensor's $PM_{2.5}$ readings in the second co-location test against the median of all four sensors, with 1:1 line as reference.*

Again, the data points are clustered close to the 1:1 reference line, except for in the case of sensor 2, where the points consistently fall below the line. It is not known what caused this result.

It should be noted that the R^2 values labelled on each linear regression plot are consistently very high, but this does not necessarily indicate the result is good. The inter-comparison tests would ideally be performed in a laboratory environment over equal periods of time. By controlling variables such as aerosol concentration, the accuracy of the sensors could be better assessed. Comparison of a greater amount of sensors would additionally improve the confidence in the result. Nonetheless, this study concludes that the four OPC-N3 sensors were in good agreement during co-location tests before and after separation.

3.2 Indoor and Outdoor Measurements

The indoor and outdoor measurements ran for just under 10 days. Before the pairs of sensors were averaged, the times series from all sensors (fig. 19) showed a clear difference between the concentrations recorded by the two indoor sensors. The ratio of each pair of sensors was plotted over time (see appendix fig. 20). This confirmed that the two sensors inside had a higher median ratio of approximately 1.3 for all size fractions, while the two outdoor sensors had a median ratio of approximately 1 for $PM_{2.5}$ and PM_{10} and a lower median ratio of 0.9 for PM_1. However, the ratio of sensor 3 to 4 was more variable over time. In averaging the two data sets for comparison between indoor and outdoor measurements, the individual errors from each sensor will propagate, resulting in a different total error.

After the respective sensors were averaged for indoor and outdoor measurements, the average concentration was calculated for each size fraction inside and outside. As shown in table 3.1, the average outdoor concentrations were higher. The ratio between indoor and outdoor particle mass concentrations was also plotted for each size fraction (see appendix 21). The median ratio of each was calculated to be 0.37 for PM_1, 0.44 for $PM_{2.5}$, and 0.53 for PM_{10}. The ratio increased to between 2–100 during cooking and candle burning.

Table 3.1: *Average indoor and outdoor concentrations of particulate matter over approximately 10 days.*

	Indoor Average ($\mu g/m^3$)	**Outdoor Average** ($\mu g/m^3$)
PM_1	1.6281	2.1824
$PM_{2.5}$	4.5644	6.9318
PM_{10}	15.7820	18.3695

The time series of 10-minute averages of indoor and outdoor measurements showed that there were several occasions when the indoor concentration exceeded the time series. The five highest indoor concentration peaks in each size fraction occurred at the same times. In these cases, the concentrations reached between 10–48 $\mu g/m^3$ for PM_1, between 35–230 $\mu g/m^3$ for $PM_{2.5}$, and between 100–800 $\mu g/m^3$ for PM_{10}. These are highly substantial increases in comparison to the average concentrations. When comparing the times to the activity log, four of these five peaks were found to coincide with cooking events, while the fifth was during a time when candles were lit and extinguished. Wang et al. (2020) found that both professional monitors and low-cost air quality sensors in a laboratory setting barely detected when a candle was burning steadily, but had a better response once it was extinguished and larger particles were formed. In the same study, sensors were able to detect frying or grilling, but not boiling or broiling. Vacuuming was expected to result in a noticeable increase in particle mass concentration, at least in PM_{10}, but there was no significant increase during the two occasions of vacuuming during these measurements.

Out of 16 recorded cooking events, half were clearly identifiable by peaks in particle mass concentration. Four had small peaks at associated times, but these were not considered significant enough in comparison to the concentration level before and after the event. The highest overall peak occurred when both frying and boiling occurred, while the other strong peaks were caused mostly by frying. The ventilation hood above the stove was always used when cooking, although it is an old and seemingly not very effective system. Despite the largest percentage of particles generated during cooking generally being in the ultra-fine region (less than 0.1 µm) (Abdullahi et al., 2013), these results strongly indicate that the OPC-N3 sensors are capable of measuring particles associated with cooking.

Another noticeable trend in the indoor air was the concentration decrease when the apartment was empty or both residents were asleep. With minimised re-suspension from movement, PM_{10} generally settled faster than the finer particles, which is expected due to the heavier mass of these larger particles.

Considering outdoor air can enter the apartment when the door or windows are open, as well as permeate through non-mechanical ventilation in all rooms, it would be expected that trends of outdoor concentrations would appear in the inside air. There were some cases when the indoor concentrations increased without a recorded indoor activity and could be attributed to an outdoor vaping event or increased outdoor concentration, but with low confidence.

Outside, the majority of the peaks in concentration were caused by vaping. These events were characterised by sharp increases and sharp decreases in concentration, unlike the peaks due to cooking which caused a sharp increase initially, but a much more gradual decrease in concentration afterwards. In the first few days of the measurement period, there was ongoing maintenance work being undertaken outside of the apartment (within 100 m from the outdoor sensors). This included high-pressure cleaning of a drain, thought to be powered by a diesel-fuelled generator, which would produce combustion particles and precursor gases. Later, earth and pavement were dug up and re-filled using heavy machinery. The workers were also observed to be smoking cigarettes close to the apartment during this period. These sources of particulate matter could have contributed to the heightened overall concentrations between April 14–17. The time and nature of these events could not be as well detailed as the residents' own activities.

Figure 11 contains the time series for PM_1, $PM_{2.5}$, and PM_{10} concentrations indoors and outdoors, with some examples of peaks due to various activities.

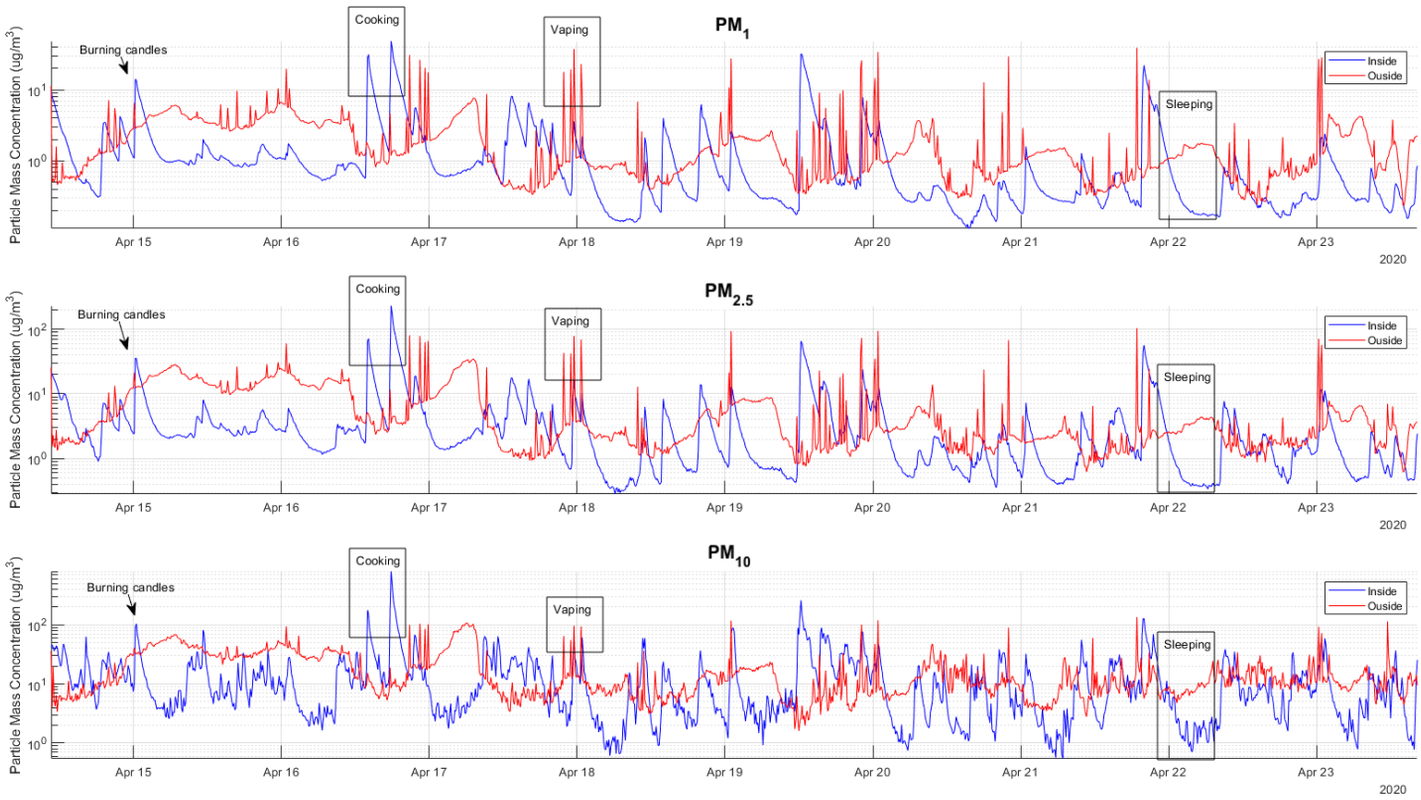

Figure 11: *10-minute averaged values of indoor and outdoor measurements. Examples of activities which produced notable increases in particle concentration are labelled.*

It was noted that the recorded temperatures, both inside and outside, were significantly higher than expected. Indoors, the average was around 30 °C, however the apartment is regulated to remain around 20 °C. The outdoor temperature time series displayed the expected diurnal variations; however, the maximum value recorded was almost 38 °C and the minimum was just above 12 °C. The air temperatures in Lund during the measurement period were at least 10 °C lower. This overestimation may arise from the lower quality of the internal temperature sensor in the OPC-N3 (the user manual cautions that the values may not accurately reflect the ambient conditions), but could also come from the electronics inside the sensor casing heating up. Furthermore, the outdoor sensor set-up was exposed to direct sunlight during some periods of the measurements.

Given the sensor's sensitivity to humidity, extra heating that in turn reduces humidity could actually be a desired side-affect. Other studies have found the reliability of OPC-N sensors is affected in conditions above 80% humidity, but the maximum RH recorded by the internal humidity sensors during these measurements was 47%. However, the true ambient RH could be underestimated by the lower quality of the internal sensor, or the localised heating within the sensor casing. Since the indoor sensors were located relatively close to the bathroom, times of showers were recorded in case the increased humidity affected the particle mass concentration. Ultimately, no obvious increases associated with showering events were found and inside concentrations did not appear to be dependent on

humidity (see appendix fig. 22). However, when the outdoor data was plotted against RH in figure 12, there did seem to be a correlation between high RH and increased particle mass concentration.

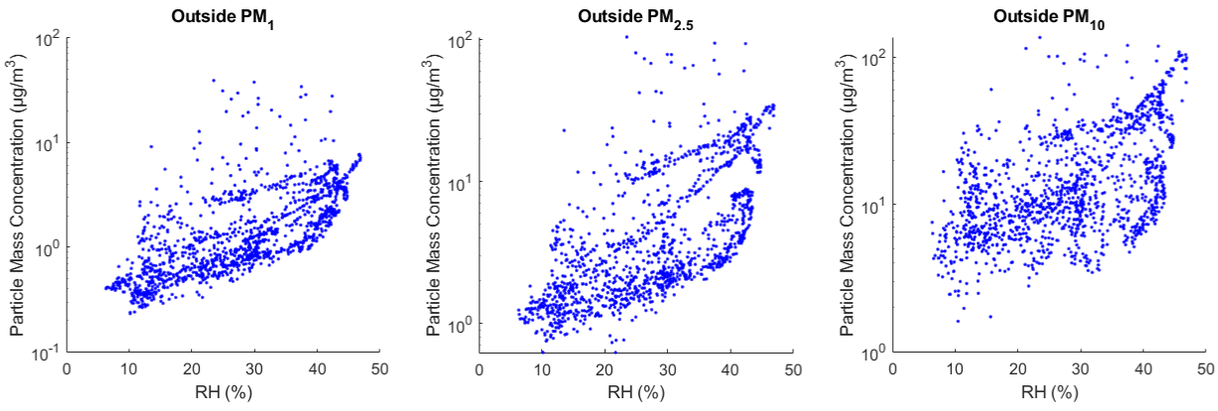

Figure 12: *Particle mass concentrations of outdoor PM_1, $PM_{2.5}$, and PM_{10} as a function of relative humidity.*

The RH sensitivity issue could be further explored by colour-coding the data points by time, in order to assess if the relationship changes during daytime and nighttime. Furthermore, a more accurate external RH sensor and testing in a laboratory environment would give a more accurate assessment of the humidity effect. RH correction factors have been developed for the OPC-N3 through studies such as Crilley et al. (2018) but were not applied in this study. Alphasense is reportedly planning to offer built-in temperature and humidity compensation in the future. A heated inlet design has also been tested for the OPC-N2 model to reduce the RH of air before sampling (Czernicki and Kallmert, 2019). Measuring dry particles is desirable since high RH causes hydroscopic growth which alters the properties of aerosol particles, making it more difficult to interpret changes in particle mass concentration.

3.3 Comparison to Reference Data

Despite the OPC-N3 sensors not being co-located with the TEOM instrument used for monitoring the PM_{10} concentration in Lund, they showed relatively good agreement, as seen in figure 13. A scatter plot of OPC sensor data against TEOM measurements showed data was scattered around the 1:1 reference line, despite the linear regression coefficients not being particularly desirable (see appendix 23).

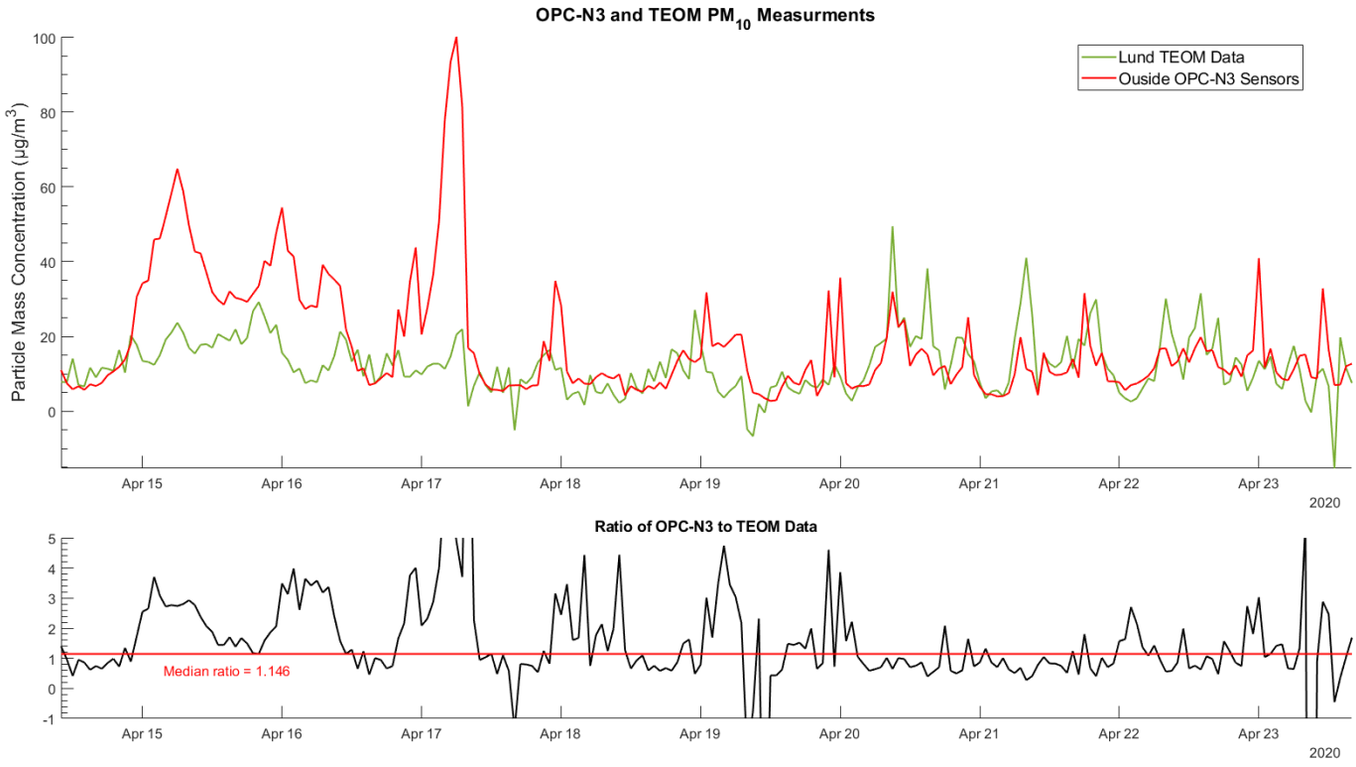

Figure 13: *Hourly averaged comparison of PM_{10} concentrations measured by outdoor OPC-N3 sensors and Lund Municipality's TEOM, and the ratio between the TEOM and the outdoor sensors (y-axis is zoomed to range -1–5) with the median ratio shown.*

During the first few days of the comparison (April 15–17), the PM_{10} concentrations measured by the OPC-N3 were significantly higher, with peaks occurring in the late evening to early morning. The TEOM did measure peaks around the same times, but the average values from the outdoor OPCs registered values that were 2–4 times higher. It was originally thought that the higher values recorded by the OPC could be a result of the construction work or vaping events, however the timing did not fit. Since these peaks occurred in the late evening to early morning, it is suspected that increased RH or reduced mixing ratio contributed to the higher values although no conclusion was reached. The ratio of the outdoor sensors to the TEOM data shows better agreement between the two datasets in the later part of measurements. Negative data from the TEOM and very high values from the outdoor sensors caused the ratio to reach large values in some cases, but the median ratio was calculated to be 1.146.

It should be noted that the PM_{10} measurements from Lund are not absolutely reliable either. The estimated uncertainty of the 1-minute TEOM is $\pm$ 2 µg/m^3, which can be compounded when taking 10-minute averages. The uncertainty comes firstly from the lack of a FDMS unit, so semi-volatile components of particulate matter may not be measured. The data is reported to the public in near–real time with the correction factor $y = x * 1.19 + 1.15$ applied, but before the data is finally validated these calibration factors need to be recalculated with the volatile correction method using data from FDMS

reference instruments situated in Malmö. Additionally, the instrument cabinet is susceptible to heating from direct sunlight and the TEOM is sensitive to significant temperature fluctuations.

3.4 Uncertainties

The calibration of the OPC-N3 with PSL particles of known diameter and RI will lead to the sensor underestimating particles with different properties. Depending on the origin and type of particles, they may scatter more or less light and thus be reported differently by the sensor. For this reason, Badura et al. (2018) recommends the re-calibration of low-cost sensors in the actual measurement environment with higher-grade instruments.

The placement and orientation of the sensor units may have led to some systematic errors. Alphasense recommends the fan exhausts into an unconstrained space to maintain uninterrupted air flow, however with the addition of two Arduino boards and attached shields and wires, the electrical boxes became rather crowded. An inter-comparison test could be performed with this set-up in one box, and another box containing only the sensors, to assess the effect on the data; alternatively using a larger casing would provide a simple solution.

During analysis, it became evident that there were some missing lines of data where some seconds were not recorded to the SD card. Closer analysis showed this occurred randomly on all four sensors. This was accounted for by using the Matlab 'resize' function and filling in the missing rows with 'NaN' (blank) values. The percentage of missing values for each sensor varied between 0.25–1.10% (appendix table 5.1). This is most likely attributed to the Arduino counter and the RTC falling out of synchronisation, or the serial communication (which has no built-in error-handling) temporarily failing. The percentage of missing rows seemed to increase with increased measurement time when comparing the length of each co-location test and the indoor/outdoor measurement. Regardless, the percentage of overall missing data was deemed to be insignificantly low. This could become an issue if shorter time resolution of measurements is required. For example, Koivisto et al. (2019) mentions that due to the substantial temporal variability of indoor settings, source identification often requires measurements on the scale of minutes. Additionally, with its default settings the OPC-N3 is not programmed to operate continuously over long periods of time. It would be interesting to explore whether these errors compound over several weeks or months of continuous measurements.

Chapter 4

Conclusions

Low-cost sensors for particulate matter are quickly emerging as promising instruments to complement existing reference and equivalent air quality monitoring methods. In this study, the optical sensor OPC-N3 from Alphasense has demonstrated close agreement between three of four co-located sensors. The precision of the sensors was worse at high mass concentrations of particulate matter, and also suffered at low concentrations (particularly for PM_{10}).

OPC-N3 sensors measured indoor and outdoor particulate mass concentrations over 10 days, and demonstrated an ability to detect changes in concentration associated with various residential activities. The sensors reported significantly higher mass concentrations of PM_1, $PM_{2.5}$, and PM_{10} during periods of cooking, burning candles, and vaping outside. Even though particles generated in such activities are typically smaller than the lower detection limit of the OPC-N3 and are thus likely underestimated, the trends detected are still indicative of the usefulness of the sensor.

Comparison of the OPC-N3 data to PM_{10} concentrations measured by a TEOM showed some correlation of trends despite the instruments not being co-located. Considerable variations in the ratio could not be explained without further investigation.

Chapter 5

Outlook

The results of this paper highlight opportunities for further research into the indoor and outdoor applications of the OPC-N3. A more comprehensive evaluation of trends could be gained by extending the measurement period, since this study was relatively short. It would be preferable to take indoor and outdoor measurements over a longer period of time, to evaluate if the sensors react to seasonal variations, or suffer loss in efficiency due to continuous measurements.

Furthermore, one of the commonly quoted attractive qualities of low-cost sensors is their ability to increase spatial resolution of measurements. It would therefore be interesting to compare the results of sensors in different rooms of a building for example, to see how well different particulate matter concentrations can be resolved on a very local scale. Moreover, since the outdoor sensors were located in a quiet residential area, not close to heavily-trafficked roads, this study cannot evaluate the sensors' performance in congested urban environments where particulate matter concentrations would be higher.

It is recommended that to further assess how accurately the OPC-N3 can measure changes in indoor air quality, single activities could be replicated in a controlled laboratory environment, similar to a study by Wang et al. (2020). There are an additional number of indoor origins of particulate matter which either were not present or not recorded in this study (including pet dander, cosmetic aerosols, cleaning sprays, or brewing coffee). Furthermore, the OPC-N3 results could be compared with instruments capable of detecting particles in the submicron size distribution, to assess how much the OPC underestimates concentrations of smaller particles.

Finally, while the addition of the Arduino microcontroller to the OPC-N3 may increase the total cost of using the sensor, it does extend the possibilities of the OPC's application, especially since the OPC-N3 can work with other slave devices on the SPI bus, unlike the previous model. Electronic modules such as motion sensors could be interesting for future indoor air studies. Futhermore, the data logger shield user-programmable LEDs were programmed to light up when an error occurred, but this was not visible when the sensors were in the casing. The Arduino could potentially be connected with a wifi module for wireless data transfer. This could allow for real-time results and also avoid interrupting the sensor set-up when collecting data. However, this would add to the cost and also limits where the sensors could be used.

During field measurements, power interruptions tend to occur more frequently, causing larger gaps in data. The addition of the RTC means the time and duration of these outages can more accurately be known and accounted for in post-measurement analysis. Timestamps also made synchronising several data sets easier in comparison to peak-matching. However, further modification to the Ardiuno sketch is required to better handle power failures, should they occur. The inherent start-up errors were removed manually in analysis, however the Arduino could be programmed to begin writing to a new file on the SD card in such a case.

Bibliography

Abdullahi, K. L et al. (2013). "Emissions and indoor concentrations of particulate matter and its specific chemical components from cooking: A review". *Atmospheric Environment* 71, pp. 260–294. DOI: 10.1016/j.atmosenv.2013.01.061.

Acharya, R. (2017). *Satellite Signal Propagation, Impairments and Mitigation*. Academic Press. Chap. 3, pp. 57–86. ISBN: 9780128097328. DOI: 10.1016/B978-0-12-809732-8.00003-X.

Alphasense (2018). *Alphasense Particle Counter OPC-N Range Product Update*. URL: www.alphasense.com/WEB1213/wp-content/uploads/2019/02/OPC-N3-information-update-Dec-18.pdf (visited on 05/01/2020).

Badura, M. et al. (2018). "Evaluation of Low-Cost Sensors for Ambient PM2.5 Monitoring". *Journal of Sensors*. DOI: 10.1155/2018/509654.

Bulot, F.M.J. et al. (2019). "Long-term field comparison of multiple low-cost particulate matter sensors in an outdoor urban environment". *Scientific Reports* 9(7497). DOI: 10.1038/s41598-019-43716-3.

Concas, F. et al. (2019). "A Gap Analysis of Low-Cost Outdoor Air Quality Sensor In-Field Calibration". *arXiv*. DOI: 1912.06384.

Crilley, L.R. et al. (2018). "Evaluation of a low-cost optical particle counter (Alphasense OPC-N2) for ambient air monitoring". *Atmospheric Measurement Techniques*, p. 709. DOI: 10.5194/amt-11-709-2018.

Czernicki, P. et al. (2019). "Evaluation of a heated inlet to reduce humidity induced error in low-cost particulate matter sensors". MA thesis. Lund, Sweden: Lund University.

Earl, Bill (2020). *Adafruit Data Logger Shield*. URL: https://learn.adafruit.com/adafruit-data-logger-shield/overview (visited on 01/28/2020).

European Commission (Sept. 2003). "Indoor air pollution: new EU research reveals higher risks than previously thought". *European Commission*. URL: https://ec.europa.eu/commission/presscorner/detail/en/IP_03_1278.

European Environment Agency (2016). *Air quality standards under the Air Quality Directive, and WHO air quality guidelines*. URL: www.eea.europa.eu/themes/data-and-maps/figures/air-quality-standards-under-the (visited on 04/02/2020).

Feinberg, S. et al. (2018). "Long-term evaluation of air sensor technology under ambient conditions in Denver, Colorado". *Atmospheric Measurement Techniques (Discussions)*. DOI: doi.org/10.5194/amt-2018-12.

Hinds, W. C. (1982). *Aerosol Technology*. United States of America: John Wiley & Sons, Inc.

Holstius, D. et al. (2013). "Field calibrations of a low-cost aerosol sensor at a regulatory monitoring site in California". *Atmospheric Measurement Techniques Discussions* 7. DOI: 10.5194/amtd-7-605-2014.

Ingebrethsen, Bradley J. et al. (2012). "Electronic cigarette aerosol particle size distribution measurements". *Inhalation Toxicology* 24(14), pp. 976–984. DOI: 10.3109/08958378.2012.744781.

Intergovernmental Panel on Climate Change (2013). *Climate Change 2013 The Physical Science Basis*. Intergovernmental Panel on Climate Change. ISBN: 978-92-9169-138-8.

Karagulian, F. et al. (2019). *Review of sensors for air quality monitoring*. Luxembourg: Publications Office of the European Union. DOI: 10.2760/568261.

Klepeis, N.E. et al. (2001). "The National Human Activity Pattern Survey (NHAPS)". *Journal of Exposure Analysis and Environmental Epidemiology* 11(3). DOI: 10.1038/sj.jea.7500165.

Koivisto, A.J. et al. (2019). "Source specific exposure and risk assessment for indoor aerosols". *Science of the Total Environment*, pp. 12–24.

Njalsson, T. et al. (2018). "Design and Optimisation of a Compact Low-cost Optical Particle Sizer". *Journal of Aerosol Science* 119, pp. 1–12. DOI: 10.1016/j.jaerosci.2018.01.003.

Samset, B. H. et al. (2018). "Climate Impacts From a Removal of Anthropogenic Aerosol Emissions". *Geophysical Research Letters* 45(2), pp. 1020–1029. DOI: 10.1002/2017GL076079.

Swedish Standards Institute (2020). *Ambient air - Standard gravimetric measurement method for the determination of the PM10 or PM2,5 mass concentration of suspended particulate matter*. URL: www.sis.se/api/document/preview/101990/ (visited on 05/07/2020).

Valavanidis, A. et al. (2008). "Airborne Particulate Matter and Human Health: Toxicological Assessment and Importance of Size and Composition of Particles for Oxidative Damage and Carcinogenic Mechanisms". *Journal of Environmental Science and Health, Part C* 26(4), pp. 339–362. DOI: 10.1080/10590500802494538.

Wang, Z. et al. (2020). "Performance of low-cost indoor air quality monitors for PM2.5 and PM10 from residential sources". *Building and Environment* 171. DOI: 10.1016/j.buildenv.2020.106654.

WHO (2006). *Air quality guidelines. Global update 2005*. Copenhagen, Denmark: World Health Organization. ISBN: 92-890-2192-6.

World Health Organization (WHO) (2016). *Ambient air pollution: a global assessment of exposure and burden of disease*. World Health Organization, p. 121.

Yuval, H.M.M. et al. (2019). "Application of a sensor network of low cost optical particle counters for assessing the impact of quarry emissions on its vicinity". *Atmospheric Environment* 211, pp. 29–37. DOI: 10.1016/j.atmosenv.2019.04.054.

Appendix

Figure 14: *Two OPC-N3 sensors connected to Arduinos and data logging shields inside the plastic casing.*

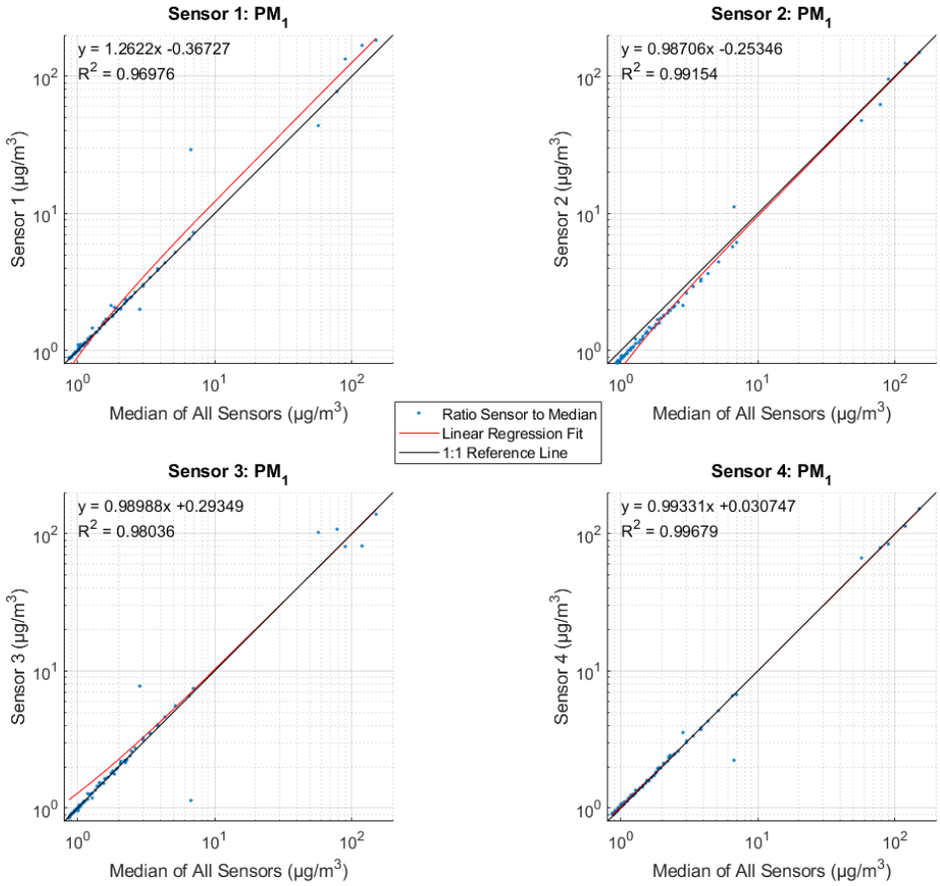

Figure 15: *Linear regression fit of each sensor's PM_1 readings in the first co-location test against the median of all four sensors, with 1:1 line as reference.*

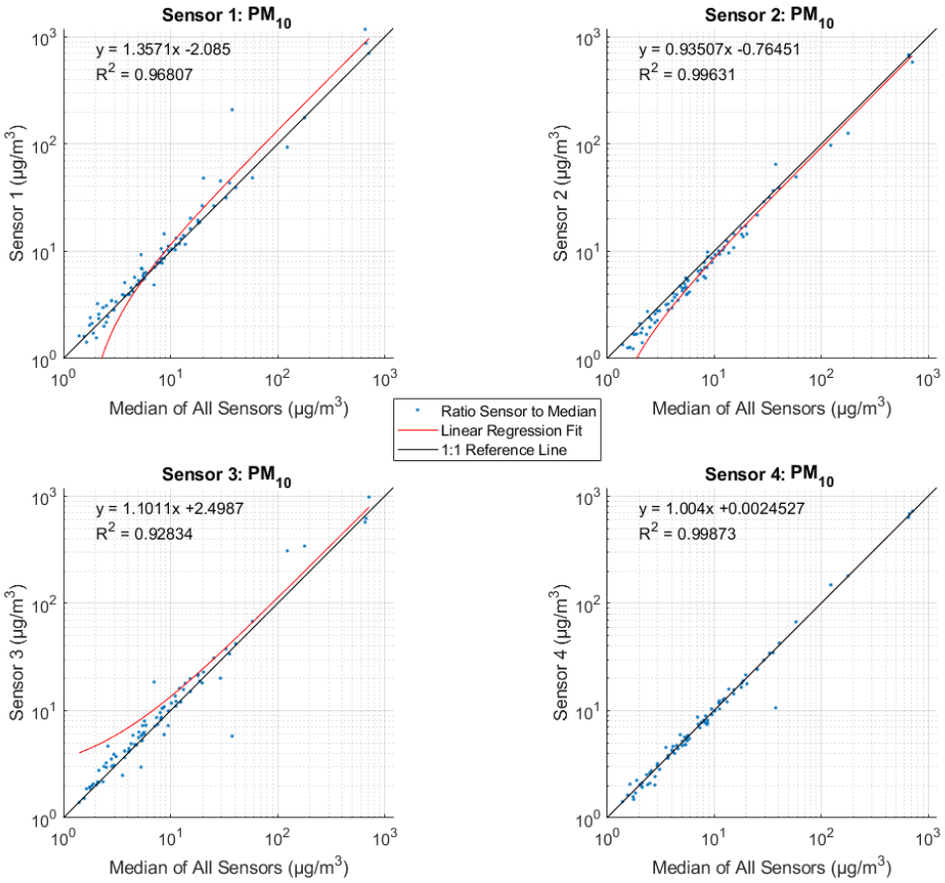

Figure 16: *Linear regression fit of each sensor's PM_{10} readings in the first co-location test against the median of all four sensors, with 1:1 line as reference.*

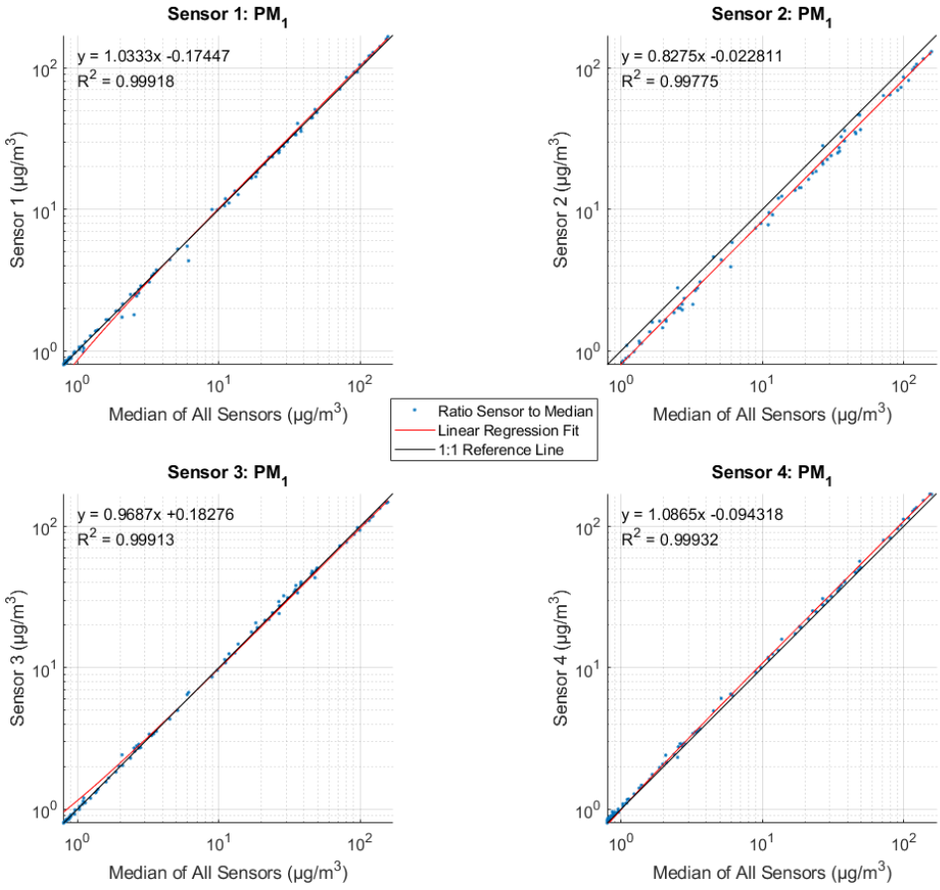

Figure 17: *Linear regression fit of each sensor's PM_1 readings in the second co-location test against the median of all four sensors, with 1:1 line as reference.*

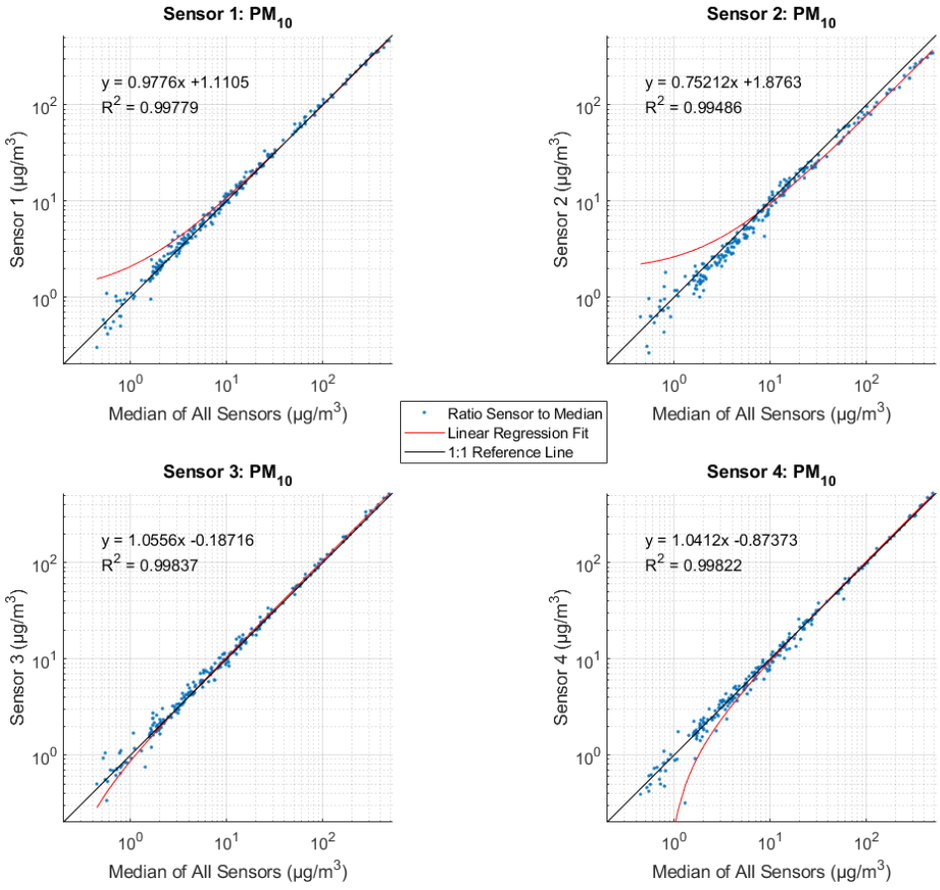

Figure 18: *Linear regression fit of each sensor's PM_{10} readings in the second co-location test against the median of all four sensors, with 1:1 line as reference.*

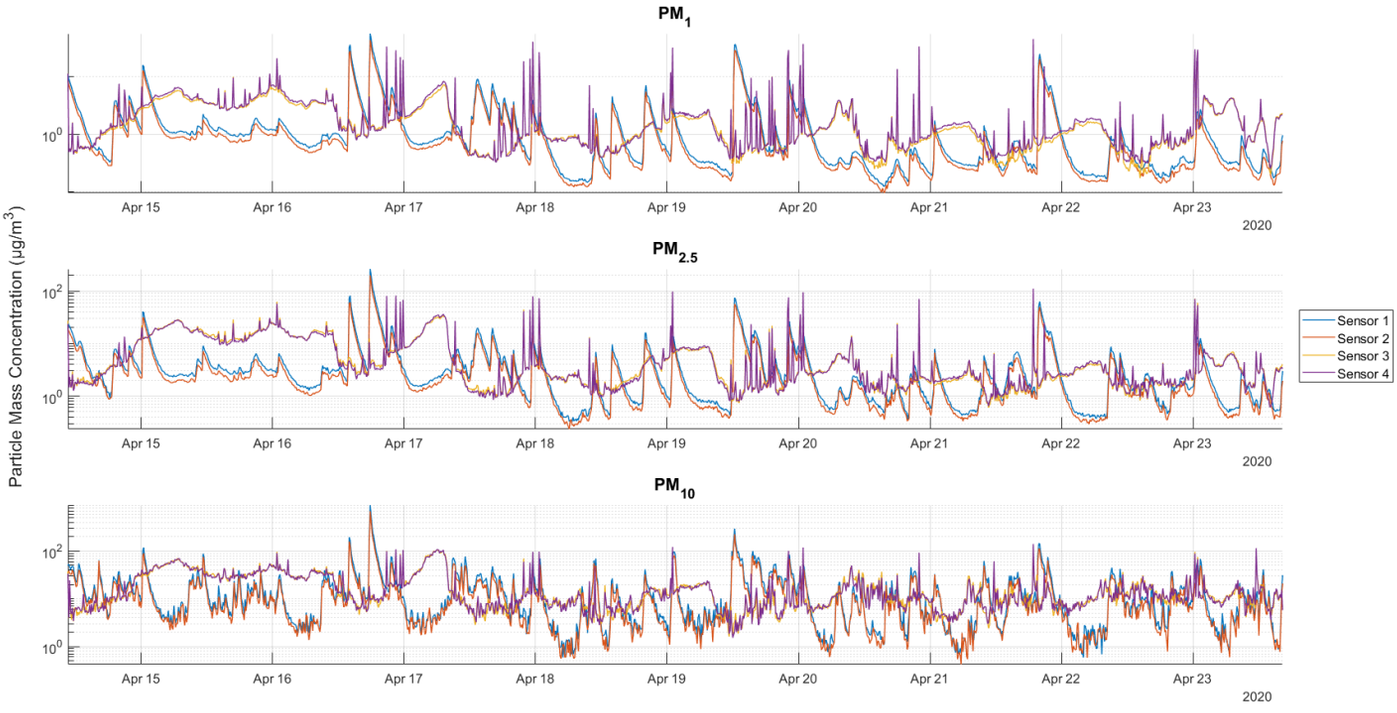

Figure 19: *Time series of all four sensors with 10-minute averages during inside and outside measurements prior to averaging the pairs of sensors.*

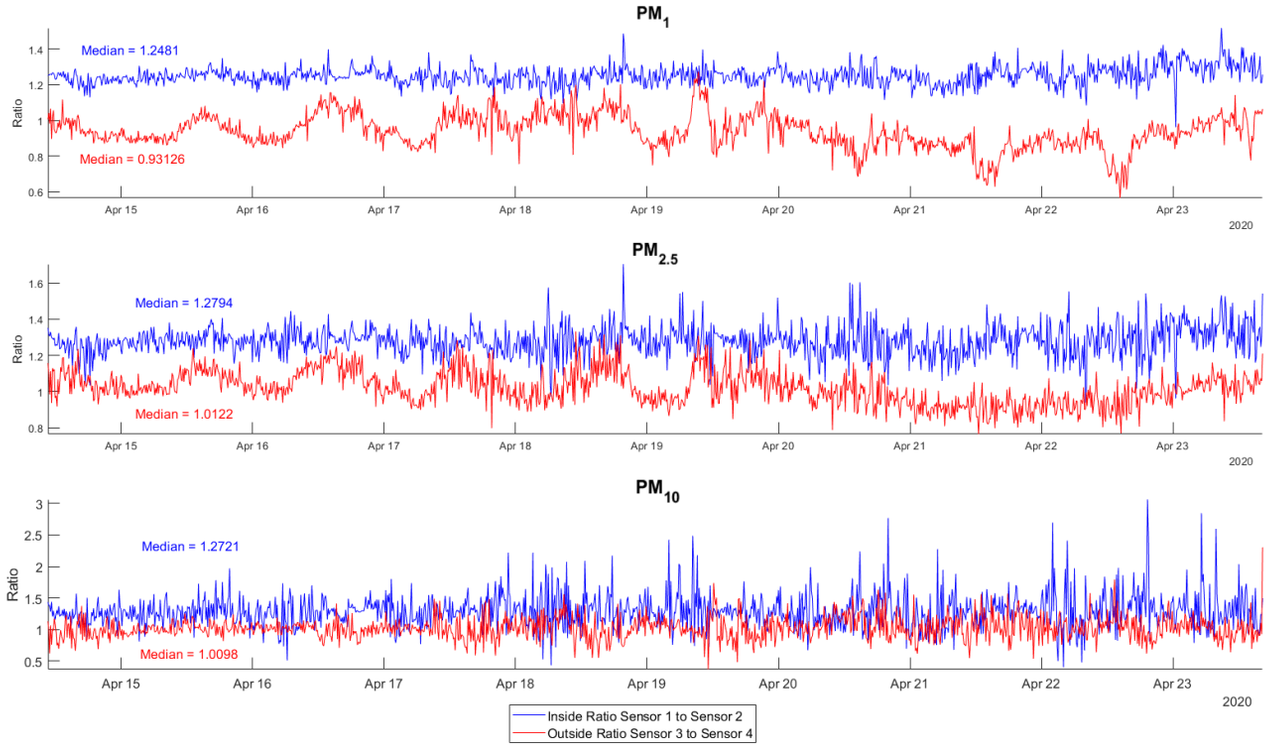

Figure 20: *Ratio of sensor 1 to sensor 2 (inside) and sensor 3 to sensor 4 (outdoors) throughout the measurement period.*

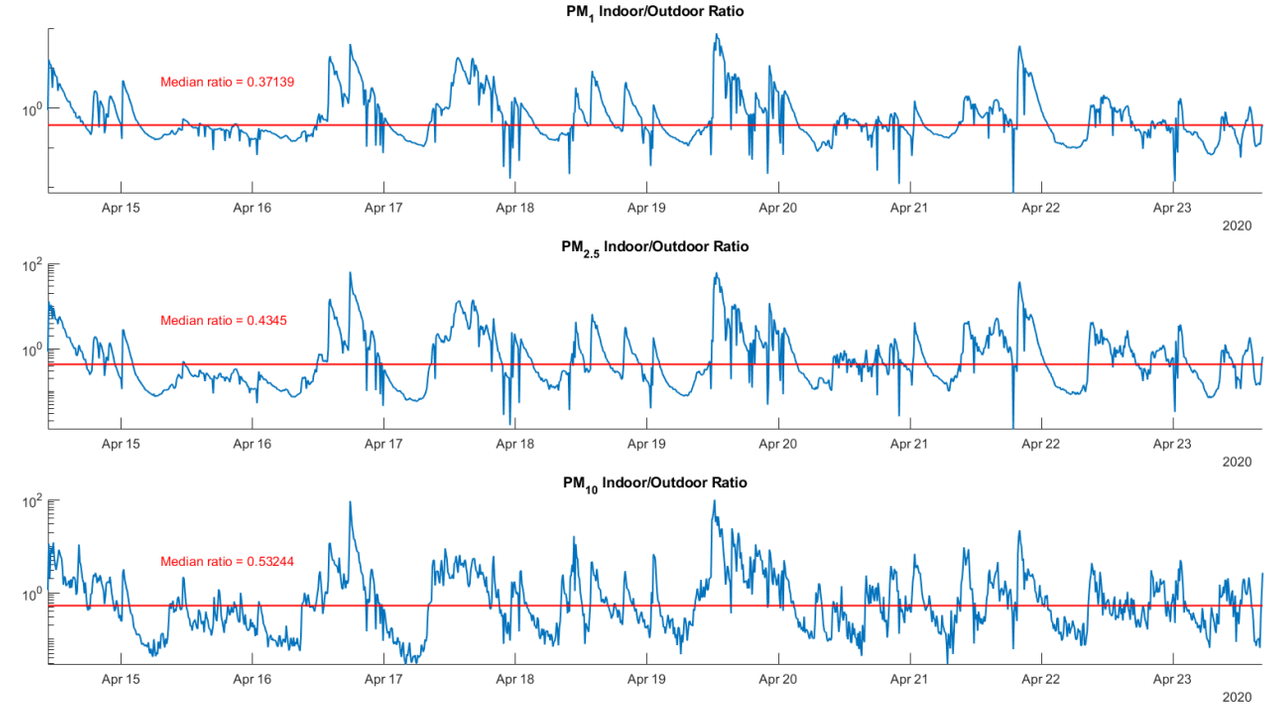

Figure 21: *Indoor/outdoor ratios for PM_1, $PM_{2.5}$, and PM_{10}.*

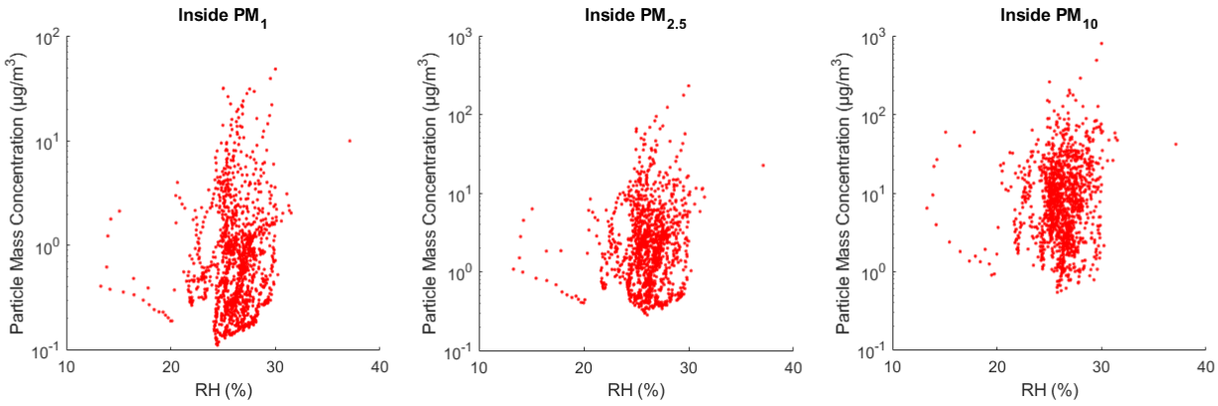

Figure 22: *Particle mass concentrations of indoor PM_1, $PM_{2.5}$, and PM_{10} as a function of relative humidity.*

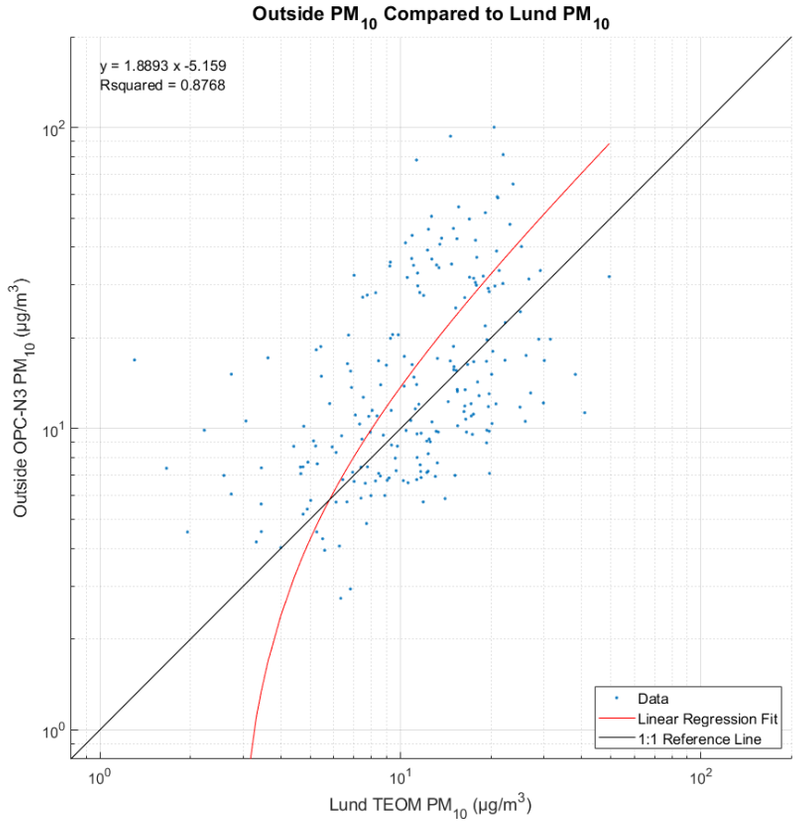

Figure 23: *Outdoor sensors compared to Lund TEOM data for PM_{10} with linear regression.*

Table 5.1: *Length of data files and number of missing rows (= number of missing seconds) for each set of measurements. The percentage of missing data is calculated.*

		Sensor 1	**Sensor 2**	**Sensor 3**	**Sensor 4**
Co-location 1	Recorded	50272	50325	50374	50328
	Missing	247	138	220	124
	Percentage	0,49%	0,27%	0,44%	0,25%
Measurements	Recorded	791430	792207	791815	790752
	Missing	7822	7550	8366	8672
	Percentage	0,99%	0,95%	1,06%	1,10%
Co-location 2	Recorded	137364	137506	137638	137513
	Missing	496	347	364	425
	Percentage	0,36%	0,25%	0,26%	0,31%